Gel electrophoresis and diffusion of ring-shaped DNA

Uri Alon* and David Mukamel
Department of Physics of Complex Systems, The Weizmann Institute of Science, Rehovot 76100, Israel
(Received 5 August 1996)

A model for the motion of ring-shaped DNA in a gel is introduced and studied by numerical simulations and a mean-field approximation. The ring motion is mediated by finger-shaped loops that move in an amoebalike fashion around the gel obstructions. This constitutes an extension of previous reptation tube treatments. It is shown that tension is essential for describing the dynamics in the presence of loops. It is included in the model as long-range interactions over stretched DNA regions. The mobility of ring-shaped DNA is found to saturate much as in the well-studied case of linear DNA. Experiments in agarose gels, however, show that the mobility drops exponentially with the DNA ring size. This is commonly attributed to dangling ends in the gel that can impale the ring. The predictions of the present model are expected to apply to artificial two-dimensional obstacle arrays [W. D. Volkmuth and R. H. Austin, Nature **358**, 600 (1992)] which have no dangling ends. In the zero-field case an exact solution of the model steady state is obtained, and quantities such as the average ring size are calculated. An approximate treatment of the ring dynamics is given, and the diffusion coefficient is derived. The model is also discussed in the context of spontaneous symmetry breaking in one dimension. [S1063-651X(97)12601-0]

PACS number(s): 87.10.+e, 36.20.Ey, 82.45.+z, 05.40.+j

I. INTRODUCTION

Gel electrophoresis is a widely used technique for separating DNA fragments according to size [1]. The separation resolution is limited by a saturation of the mobility at large DNA size. Separation of large DNA fragments has been made possible by pulsed-field gel electrophoresis [2,3]. In view of the phenomenal successes of these techniques, an analytic approach to the basic underlying motion of the molecule through the gel is desirable.

Most theoretical treatments [4–10] of the motion of the DNA through the gel are based on the reptation concept [11]. The DNA is pictured as moving through an impenetrable tube defined by the surrounding gel obstructions, with the motion mediated by a snakelike reptation of the polymer ends. Reptation has proven very successful in describing equilibrium dynamics of polymers in gels and melts. Simulations [12] and experiments [13], however, have indicated that for sufficiently long chains undergoing electrophoresis, an alternative mechanism of motion is important: the formation of finger-like loops or leaks through the reptation tube. These loops (sometimes also called hernias, hairpins, or kinks) constitute a protrusion of the DNA chain through the walls of the reptation tube in a doubled-up loop. Loops have been included in some recent simulations of linear DNA fragments undergoing gel electrophoresis [14–16]. An additional important effect, that is often neglected in treatments inspired by equilibrium reptation theory, is tension transmitted along the DNA chain [12]. Under a driving electric field, strong tension forces can dramatically affect the polymer motion [16,17].

In linear DNA chains, both loop motion and ordinary reptation of the chain ends are possible. In order to separate out and emphasize the effect of loops, here we consider DNA in the shape of a ring (open-circular DNA [18]). The DNA ring can move around the gel obstacles only by loops, sending out fingers in an amoebalike fashion. To our knowledge, there have been no theoretical studies on gel electrophoresis of open-circular DNA, despite the fact that in practical applications, ring-shaped DNA (plasmids) is often analyzed by gel electrophoresis, and shows behavior different from that of linear DNA fragments [19–22].

The behavior of ring polymers in the absence of an electric field is also of interest [23–25]. This problem is related to the behavior of a melt of ring polymers, and also to electrophoresis in the weak-field limit through an Einstein relation. The diffusion of ring-shaped polymers in a lattice of obstructions has been treated by numerical simulations and theoretical arguments [25]. An exact treatment of the statics and especially the dynamics of ring-shaped polymers in zero field is, however, not available.

In this work, a model for the motion of ring-shaped DNA in a gel is introduced and studied numerically and analytically. The ring motion is mediated by loops that finger between the gel obstructions. This model, described in Sec. II, constitutes an extension of previous reptation tube treatments. It is instructive to first study the model neglecting the effects of tension transmitted along the DNA polymer. Monte Carlo simulations of the model, summarized in Sec. III A, show that the chain mobility in this case decreases exponentially with DNA size. This is due to the formation of hooks which reduce the mobility. This behavior is modified when tension is taken into account. In Sec. III B, tension is added to the model as long-range interactions over stretched regions of the polymer. Tension increases the unhooking rates, and stabilizes a ring conformation aligned with the field. This causes the mobility of long ring-shaped DNA to saturate to a finite value, much as in the well-studied case of linear DNA. Experiments in agarose gels [19–22], however, show that the mobility drops to zero with the DNA ring size,

*Present address: Depts. of Physics and Molecular Biology, Princeton University, Princeton, NJ 08540.

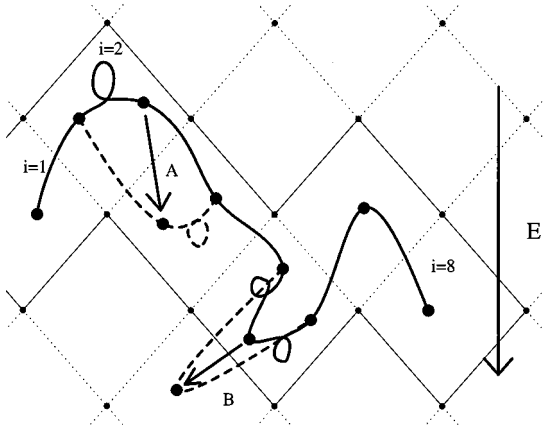

FIG. 1. Configuration of a DNA chain (heavy line) in a gel, defined by a periodic lattice of gel pores (dotted lines). The DNA is divided into persistence length segments, numbered $i=1,2,\ldots,L$ (in this case $L=8$). The reptation tube (light line) is defined by all pores through which the DNA threads. The configuration is encoded using a $+$ for segments that are stretched between two pores with the field direction, $-$ for segments stretched against the field direction, and 0 for coiled segments in the same pore. The displayed configuration is thus $-0++00-+$ for $i=1,\ldots,8$. Move A corresponds to to a standard reptation move (inside the reptation tube) $+0\rightarrow 0+$. This move occurs with rate p. The reverse move $0+\rightarrow +0$ is against the field direction, and is given a smaller rate q. Move B corresponds to the formation of a loop (leak through the reptation tube). It is represented by pair creation $00\rightarrow +_{\sqcup}-$.

with large rings hardly penetrating into the gel. This is commonly attributed to the rings becoming impaled on dangling ends or other impurities in the gel. The predictions of the present model are expected to apply to artificial two-dimensional obstacle arrays [28] which have no dangling ends. In Sec. III C, the polymer motion is qualitatively described by a mean-field treatment. In the zero-field case, discussed in Sec. IV, an exact solution of the model steady state is obtained, and quantities such as the average ring size are calculated. In Sec. IV B, an approximate treatment of the zero-field ring dynamics is given, and the diffusion coefficient is derived. This gives an analytic foundation to previous scaling arguments [25], and suggests a framework for analysis of dynamical features of driven polymers. In Sec. V, the model is also discussed in the context of spontaneous symmetry breaking in one dimension.

II. MODEL FOR DNA IN A GEL INCLUDING LOOPS

We present a model for a charged polymer ring moving in an electric field in an array of obstacles (e.g., a gel). The model is based on the Rubinstein-Duke (RD) approach [7–9], and is extended here to include loops, which are hairpin-shaped excursions out of the usual reptation tube. Loops are crucial for polymers in the shape of a ring, in which the motion through the surrounding obstacles may be accomplished only by loop fingering.

We begin by describing the RD model for reptating linear polymers. We then extend the model to include loops. In the RD model, the gel is idealized as a lattice of point obstacles, with pore diameter b, as shown in Fig. 1. In agarose gels, $b\sim 100$ nm, while in recently introduced artificial obstacle arrays $b\sim 1\,\mu$m [28]. The DNA is represented as a chain of L segments, each of one persistence length (~ 50 nm). The segments may be stretched, when the polymer threads through adjacent pores, or coiled, when the segment is contained in one pore. Each configuration of the polymer is represented by the positions of the successive cells that the polymer threads. A simplified description of the chain is coded by the projection along the field direction of the displacement between segment ends. This displacement can be either $+b$, when the segment threads between two pores in the field direction, $-b$ when it threads two pores against the field direction, or 0 when the segment is coiled in one pore. Thus the configuration is reduced to a one-dimensional lattice of L sites. Each site i corresponds to a DNA segment, and has a state ϕ_i, which can be $+$, $-$, or 0, as demonstrated in Fig. 1. Note that in this description some information regarding the microscopic configuration is lost. However, it provides a convenient way to model the dynamics [7–9].

The chain reptates by the motion of the coiled, lax segments through the chain. In an aquaeos solution, the DNA is assumed to be uniformly charged. The forces acting on each segment are an electric force $F_e=QE$, where Q is the charge per segment and E is the field strength, and a thermal Brownian noise $F_{\rm th}$ of the order of kT/b. These forces are represented in the model by the following rules. At each time step, a pair of sites is chosen at random, and a move is made with the following rates:

$$+0\rightarrow 0+ \text{ at rate q}, \quad 0+\rightarrow +0 \quad \text{at rate p}, \tag{1}$$

$$-0\rightarrow 0- \text{ at rate p}, \quad 0-\rightarrow -0 \quad \text{at rate q}, \tag{2}$$

while $+-$ or $-+$ pairs are stuck, since they represent two stretched segments hooked around a gel obstacle (see Fig. 1). Moves in the field direction are favorably biased over the reverse moves, through the rates p and q. These rates are determined, in the case of weak fields, by local detailed-balance conditions [8], such as

$$p=\omega_0 \exp(\epsilon/2), \tag{3}$$

$$q=\omega_0 exp(-\epsilon/2), \tag{4}$$

where ω_0 is a microscopic rate and $\epsilon=QEb/kT$. Note that this is a nonequilibrium dynamics and that it does not obey full detailed balance. The ratio between these rates is thus a Boltzmann factor of the ratio of electrical to thermal energy,

$$p/q = = exp(\epsilon), \quad \epsilon=QEb/kT. \tag{5}$$

These rules, along with rates for injection of $+$ and $-$ at the head and tail of the linear chain, define the Rubinstein-Duke model [8,9].

We now extend this model to account for loops. A loop amounts to a projection of the chain from a pore with at least two coiled segments (two adjacent 0 sites) into a new pore, threading one segment out of the pore and another segment back to the original pore (for example, move B in Fig. 1). This corresponds to a pair creation move $00\rightarrow +-$. The reverse annihilation move $+-\rightarrow 00$ corresponds to the loop

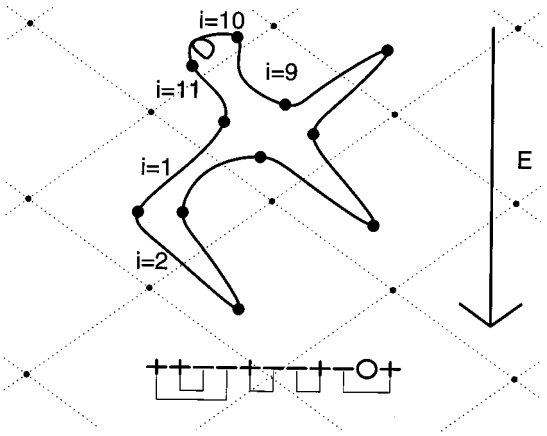

FIG. 2. A configuration of a ring-shaped DNA in the gel. The segments are numbered counterclockwise. The configuration contains several branching fingers, and is encoded as shown by a string of $+$, $-$, and 0's along with their pairings into loops. Ring-shaped DNA can move through the gel only by the annihilation and creation of loops.

retracting and forming two coiled segments in a single pore. After a pair is created, $+$ and $-$ can diffuse according to the RD rules. An important feature of the model is that pairs of $+$ and $-$, which are created together, are tracked as a connected pair throughout the dynamics. Each $+$ in the configuration has a unique $-$ to which it is connected. Keeping track of such connections between pairs is necessary in order to track the loop finger hierarchy. To see this, consider a pore with many coiled segments. A number of loops may be formed, projecting into different neighboring pores. An important point is that $+$'s and $-$'s from different loops cannot annihilate (assuming that several loops originating from the a pore always project to different neighbors, a reasonable assumption for pore lattices of high coordination number). Thus pairings of $+$'s and $-$'s must be tracked: each $+$ can annihilate only with the unique $-$ to which it is paired. Each configuration is defined by the $+$ and $-$ and 0 sites, along with their pairing to loops (Fig. 2). Only pairings in which the hernia pairs are nested are allowed, as shown in Fig. 3 (pairing lines may not cross each other). Starting with an allowed configuration, the loop creation rules assure that the configuration at each subsequent time is also allowed. The phase space is larger than in the original

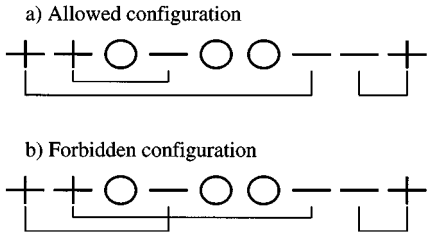

FIG. 3. An example of a configuration of $+,-$, and 0 charges in the model. (a) One of the allowed pairings into loops. (b) A forbidden pairing, where the loops are not nested. Such a configuration cannot be reached from an allowed configuration by the model dynamics.

RD model which has the three states $+$, $-$, and 0 for each site, but no pairings.

The loop creation and annihilation moves, which supplement the reptation moves of Eqs. (1) and (2), are

$$00 \rightarrow +_{\sqcup} - \text{ at rate } c, \quad 00 \rightarrow -_{\sqcup} + \text{ at rate } c', \tag{6}$$

$$+_{\sqcup} - \rightarrow 00 \text{ at rate } a, \quad -_{\sqcup} + \rightarrow 00 \text{ at rate } a'. \tag{7}$$

The symbol $_{\sqcup}$ denotes pairs of $+$ and $-$ that have been created together (connected pair). The loops tend to grow, as the field bias pushes the $+$'s to the left and, the $-$'s to the right. The loops may develop subloops, and a hierarchy of loops may form. An example is shown in Fig. 2 for a ring-shaped polymer. Thus the polymer can assume a highly ramified shape, with a hierarchy of loops of different sizes.

The model as described above neglects an important physical effect: the tension transmitted along the chain. As shown below, this proves to be very important in the electrophoresis of ring-shaped DNA. Tension acts as a long-range effective interaction, and is included in the model as described in Sec. III B.

III. GEL ELECTROPHORESIS OF OPEN-CIRCULAR DNA

Using the model, we studied gel electrophoresis of ring-shaped (open circular [18]) DNA. Periodic boundary conditions are thus imposed in the model. The ring is not concatenated with any gel obstacle (it is prepared outside the gel and moves into the gel under the field influence). We first study the model in the absence of tension by Monte Carlo simulations. The treatment of tension, and its effects on the dynamics, are presented in Sec. III B. A simple mean-field treatment is given in Sec. III C.

A. Monte Carlo results

It is instructive to first study the model as described in Sec. II, neglecting the effects of tension. In order to investigate the model, we performed Monte Carlo simulations, typically using $a=c=1$, $a'=p$, $c'=0$, $p/q=1.01-2$, and ring lengths up to $L=100$. The mobility as a function of time is shown in Fig. 4. It is seen, that the mobility displays a spiked behavior: the system is effectively in one of two states: one with a positive mobility, and one with a zero mean mobility. The average lifetime of the zero-mobility states grows as L increases.

The nature of the dynamics is clarified by snapshots of the ring configurations in the two states, shown in Fig. 5. It is seen that the ring cycles between quasilinear and hooked states. The high-mobility phases correspond to the quasilinear conformation in which the ring is aligned with the field [29]. The conformation of effective charges in the model that represents this conformation is shown in Fig. 6(a). This conformation is short lived, because it develops an instability: a loop that buds on the side of the quasilinear ring grows into a hooked configuration with two stretched arms, pinned over an obstacle [see Fig. 6(b)]. In this phase, the ring is stuck, and there is zero mean mobility. The hooked state persists for a long time. The ring unhooks by one of the arms retracting by fluctuations, until a new, quasilinear, high-mobility shape is attained. This explains the burstlike structure of the

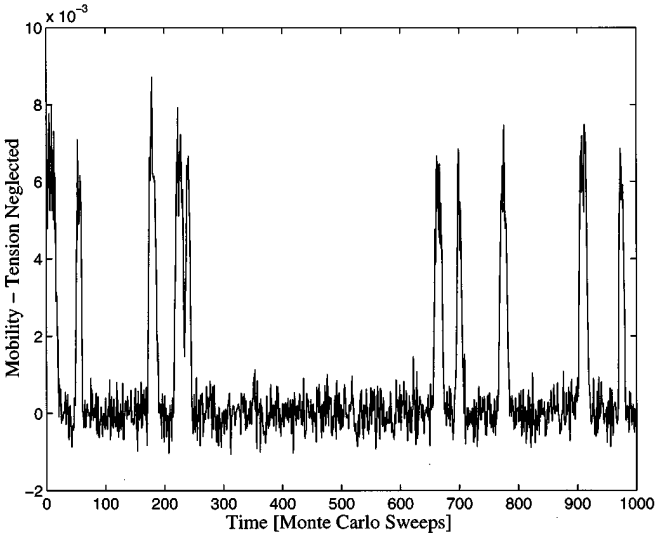

FIG. 4. Monte Carlo simulation results of the model including loops but neglecting tension, for a ring of size $L=52$, with $p=0.56$, $q=0.5$, and $c=a=1$. The mobility of the ring (center of the mass velocity) is shown as a function of time (in sweeps, where one sweep equals L single-bond moves). The mobility is seen to have a spiked behavior, where the mobility is mostly zero with intermittent periods of motion.

mobility. In the absence of tension, the mean mobility μ decreases exponentially with L (Fig. 7). This is because the unhooking rate, by which an unstretched segment moves from one arm to the other, is exponentially small, since it takes on the order of L steps against the field for the segment to escape the arm's effective potential trap. Similar dynamics can also occur in linear chains [12,16]. In the unhooking

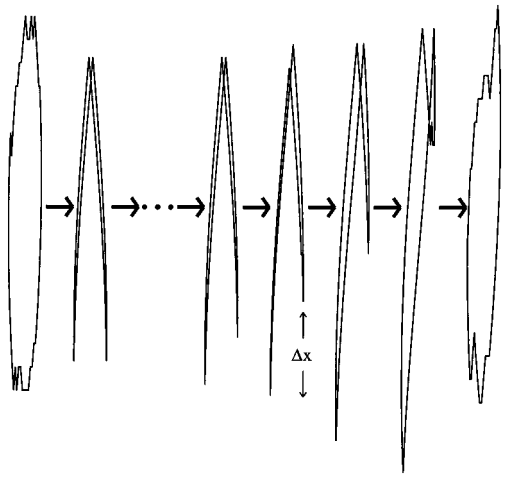

FIG. 5. The ring configurations between one mobile burst and the next. The ring begins with a quasilinear shape aligned with the field, which quickly develops an instability to secondary loops and goes to a two-armed hook. The hooks (in the absence of tension) are stuck for long times. Unhooking occurs by the retraction of one of the arms by fluctuations against the field, until a quasilinear shape with a nonzero mobility is reached again. The spikes in the ring mobility in Fig. 3 are thus explained by the cycle between quasilinear and hooked conformations.

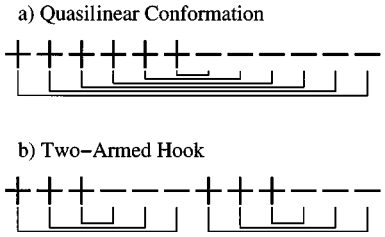

FIG. 6. Configuration of charges and loop pairings in the model that corresponds to (a) a quasilinear conformation, and (b) a hook with two equal arms. The quasilinear conformation typically also includes many 0 sites, as well as small branching subloops.

phase, tension plays a crucial role, as described in Sec. III B.

B. Effect of chain tension

It is important to consider the effects of tension transmitted along the chain [12,16, 17, 30]. The main effect of tension is to increase the unhooking rates of stretched hooks dramatically. It acts as a long-range interaction between coiled segments [16]. Tension in the context of gel electrophoresis of linear DNA was treated in a previous study [16], where coiled segments were allowed to make long-ranged hops along the chain. The present treatment simplifies this by using only local hops. In addition, the present model extends Ref. [16] by taking into account the effect of tension on the loop creation and annihilation rates.

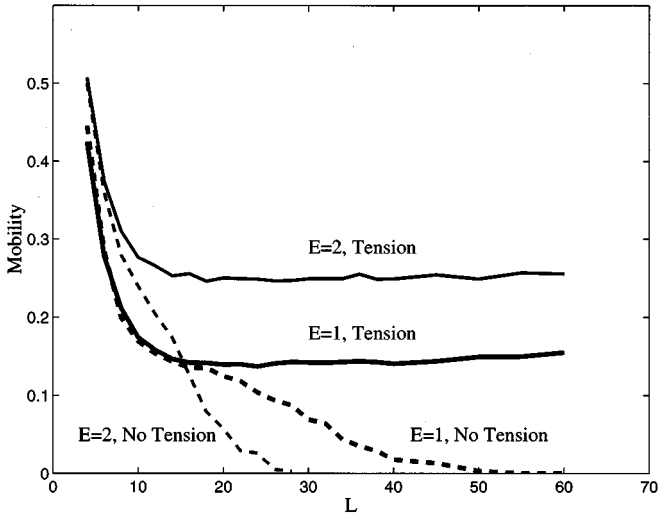

FIG. 7. Mobility of a ring-shaped DNA fragment as a function of size. Monte Carlo results for two field strengths, $E=2$ (light lines), and $E=1$ (bold lines), are shown with loop creation and annihilation rates $a=e^{-1}$ and $c=0.3$. Units are such that $Qb/kT=1$, so that the dimensionless field $\epsilon=E$. The mobility of the model including tension (full lines) decreases with the chain length for short chains, and then shows a saturation. For stronger fields, the asymptotic mobility is higher, and the chain length $L^{\star}$ at which the mobility saturates is smaller. The results of the model without tension (dashed lines) are close to the results with tension for short chains ($L<L^{\star}$). However, without tension, an exponentially decreasing mobility is predicted for long chains, because of the formation of hooks.

In order to model the effect of tension, we note that under the influence of an electric field the charged chain behaves like a chain moving in a gravitational field coupled to its weight. The tension transmitted along the chain is relaxed at coiled (0) segments and at loop tips ($+_{\sqcup}-$ and $-_{\sqcup}+$ paired at neighboring sites). Note that unpaired neighboring $+-$ or $-+$ sites represent segments of DNA chain which are draped over a gel obstruction, and therefore are capable of transmitting tension. We define an effective field for each pair of sites, which corresponds to the tension generated by regions of stretched chain on both sides of the sites. This results in a movement rate ω_j for the pair of sites j and $j+1$, which depends on long-range interaction between different sites, as described below. At each step of the simulation, a pair of sites j and $j+1$ is chosen at random. Pairs at which there is an allowed move are of three types: (a) coiled sites adjacent to a stretched site $\phi_j,\phi_{j+1}=0-,-0,0+$, or $+0$; (b) two coiled sites $\phi_j,\phi_{j+1}=00$ (creation move); or (c) a loop tip $\phi_j,\phi_{j+1}=+_{\sqcup}-$ or $-_{\sqcup}+$ (annihilation move). We will refer to such pairs as *relaxed pairs*. If the pair is not one of these three types, it remains unchanged. If the pair has an allowed move, the move is performed with the rate ω_j, and the states of sites $j,j+1$ are accordingly adjusted. A new pair is chosen and the process is repeated.

To derive the movement rate for pair j (sites j and $j+1$), ω_j, we consider the tension transmitted along the DNA due to stretched regions of chain on either side of the pair. Since the tension accumulates along these regions, the local tension field is proportional to the net displacement in the field direction of these stretched regions. The stretched regions terminate at either a coiled segment (0 site) or a loop tip, since these are the points at which the chain tension is relaxed. The effective tension force acting on a pair consisting of a coiled segment adjacent to a stretched one $(0,\phi_{j+1})$, with $\phi_{j+1}=\pm 1$, is

$$F_j=\tfrac{1}{2}\,\epsilon\sum_{m=j+1}^{k_1}\phi_m, \tag{8}$$

where k_1 is the closest succeding site to site $j+1$, which is a member of a relaxed pair, and the dimensionless external field is $\epsilon=QEb/kT$. Similarly, for a $(\phi_j,0)$ pair with $\phi_j=\pm 1$, the effective force is given by

$$F_j=-\tfrac{1}{2}\,\epsilon\sum_{m=k_2}^{j}\phi_m, \tag{9}$$

where k_2 is the closest preceding site to site j which is a member of a relaxed pair. The force acting on a loop tip ($+_{\sqcup}-$ or $-_{\sqcup}+$ pairs) is

$$F_j=\tfrac{1}{2}\,\epsilon\left(\sum_{m=j+1}^{k_1}\phi_m-\sum_{m=k_2}^{j}\phi_m\right), \tag{10}$$

with similar definitions of k_1 and k_2. (We note that the model can also be applied to linear chains, where additional points at which tension is relaxed are the chain ends.)

As an example, consider the configuration of Fig. 2. This configuration contains one coiled segment at site $i=10$, $\phi_{10}=0$. Consider sites 9 and 10, at which the configuration is -0. To evaluate the effective field for this pair, we sum ϕ in the two sites to the right of the pair (these sites cancel each other), where we reach a loop tip. The total effective force is $F_9=0$. At sites 10 and 11, where the configuration is $0+$, tension accumulates along a three-site stretched $+$ region to the right of the pair, which terminates at a loop tip, and $F_{10}=\frac{3}{2}\epsilon$.

The movement rate ω_j can be related to the local tension force F_j from a consideration of the thermal and friction forces on the string. The motion of the DNA segments through the solvent is such that viscous drag forces are much larger than any inertial term [12,17]. The behavior of the chain under thermal noise can be treated using a Fokker-Planck approach [16], using a Smoluchowski equation for the string motion along the tube contour, which includes a Brownian term and a friction coefficient proportional to the string's length. In the present work we propose a simpler physical model, which is valid at both the strong- and weak-field limits:

$$\omega_j=\begin{cases} r_j\exp(F_j), & F_j<0 \\ r_j(1+F_j), & F_j>0, \end{cases} \tag{11}$$

where r_j is equal to a microscopic rate ω_0 for pairs where a coiled segment can move $(\phi_j,\phi_{j+1}=+0,0+,0-,-0)$, $r_j=c_0$ for pairs where a loop can be created $(\phi_j,\phi_{j+1}=00)$ and $r_j=a_0$ where a loop can be annihilated $(\phi_j,\phi_{j+1}=+_{\sqcup}-,-_{\sqcup}+)$. At all other pairs of sites, $r_j=0$, since no other moves are allowed. The constants ω_0, c_0, and a_0 are the microscopic rates of the various processes. Equation (11) goes to a Boltzmann factor for low effective fields, where it represents local detailed balance. At high effective field strength, the movement rate becomes linear in the effective field strength. This is expected, since at large fields thermal fluctuations become unimportant and the local chain velocity becomes proportional to the local force [12]. Equation (11) allows loop annihilation rates to be affected by chain tension, with annihilations at loop tips flanked by long regions stretched in the field direction given a high rate.

The model without tension, described in Sec. II, can be recovered from this model, by taking $k_1=j$ and $k_2=j+1$ in Eqs. (8)–(10). This corresponds to the screening limit, when the density of coiled segments is so high that there appear no extended regions of stretched segments in which tension can develop, and the field at each bond is due to the external field alone. In this case, the movement rates are related to those of the model without tension described in Sec. II at low fields ($\epsilon\ll 1$) via $p=\omega_0 e^{\epsilon/2}$, $q=\omega_0 e^{-\epsilon/2}$, $c=c_0$, $a=a_0 e^{-\epsilon}$, $c'=c_0$, and $a'=a_0 e^{\epsilon}$. It is seen that in this limit, the rates satisfy Eq. (5).

Tension causes hooks to have a much smaller effect on the mobility. Monte Carlo calculations, including tension at two different field strengths, are shown in Fig. 7. We find that the ring mobility saturates at large DNA sizes, much as in the well-studied case of linear DNA fragments. It is interesting to note that the ring arranges itself into a quasilinear shape in the size regime studied. Here, coiled segments are very frequent—roughly one-third of the segments are coiled. Thus *tension is screened by the coiled segments* and has a very small effect during most of the dynamics, since it is important only in long, continually stretched pieces of the

chain. Only when a side-loop forms, and a hook begins to be created, does tension come into play, and essentially stabilizes the quasilinear shape aligned with the field. We note that for very large rings, branching effects similar to those discovered in large linear fragments in Ref. [16], are likely to occur, though the ring mobility should remain constant.

The screening of tension by coiled segments is very important in explaining the success of reptation tube models for linear DNA which seem to describe experiments on linear DNA fragments quite well [10,32], though the models neglect both loops and tension. The present results suggest that when including loops in a model of polymer dynamics, it is essential also to take tension into account, as these two effects have a canceling behavior, respectively increasing and decreasing the hooking rates.

The predictions of the present model that the mobility saturates with the ring size disagree with experiments. Studies of open-circular DNA (plasmids) run through agarose gels show that, above a certain DNA size, the plasmids are ''stuck at the wells'' and do not enter the gel [19–22]. The explanation offered by Mickel, Arena, and Bauer [19] is that the rings become hooked on dangling ends in the gel (unconnected ends of the gel fibers or other impurities that penetrate the pores), which impale the ring (''hoop in stick'' effect). The ring can unhook by a fluctuation which can overcome the field pulling the ring. The probability of such a fluctuation is exponentially small in the ratio between the electric force pulling the ring and the thermal forces, and the mobility is

$$\mu \sim \exp(-QENb/kT). \tag{12}$$

The saturation of the mobility predicted in the present model could be checked experimentally on recently introduced artificial two-dimensional (2D) arrays of obstacles [28] with no dangling ends that can impale the ring, as suggested in Sec. VI.

C. Mean-field treatment

In the presence of tension, the DNA is found mostly in a quasilinear conformation aligned with the field, with many coiled segments. The coiled segments essentially screen tension. This allows for a simple and local mean-field treatment of the DNA motion.

Consider a quasilinear chain (Fig. 5, rightmost and leftmost configurations). In this configuration, loops are annihilated at the upfield end of the ring. The coiled segments (0's) which are generated move down to the leading end, where a new loop is formed. The density of coiled segments, ρ, is given by a balance of loop creation and annihilation. The rates for these processes are obtained in the mean-field approximation by neglecting correlations: Loops are created (at the leading end) when two coiled segments are adjacent, at a rate $c\rho^2$, and annihilated (at the upfield end) when two stretched segments are adjacent at rate $a(1-\rho)^2$. In this approximation for the annihilation rate, the assumption that the ring is quasilinear is used, since a stretched segment can annihilate only with its unique pair. In a random configuration the pair would have a small chance of being adjacent. Here we assume that, in the quasilinear configuration, a pair of stretched segments at the leading end may always be annihilated.

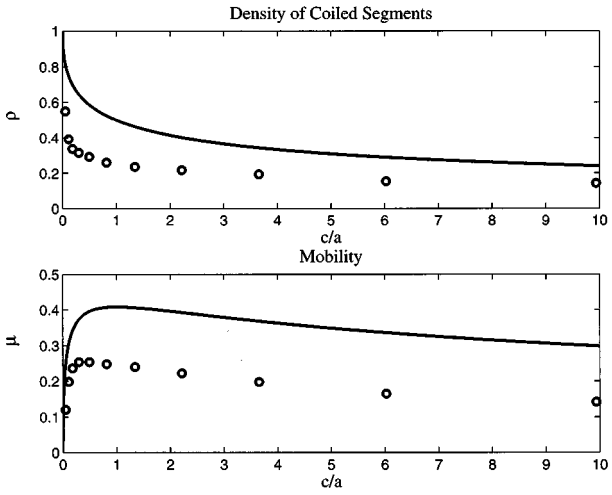

FIG. 8. Density of coiled segments, ρ, and mobility, μ, of ring-shaped DNA as a function of the ratio of loop creation and annihilation rates c/a. The ring size is $L=40$, the field strength is $E=2$, and the annihilation rate is held constant $a=e^{-1}$. Shown are Monte Carlo simulation results of the model including tension (o's), and the mean-field prediction (line).

The balance between annihilation and creation yields

$$\rho = 1/(1+\sqrt{c/a}). \tag{13}$$

The mobility μ, equal to the mean center of mass displacement per unit time, is given by an average over all the configurations allowing movement, weighted by the respective rates. Since in steady state the loop annihilation and creation moves balance each other, we have, in the simplest mean-field approximation, that the mobility is proportional to the probability of finding a stretched segment adjacent to a coiled one:

$$\mu = (p-q)\rho(1-\rho), \quad \rho = 1/(1+\sqrt{c/a}). \tag{14}$$

The qualitative features of the mobility are reasonably described by the simple mean-field theory, as shown in Fig. 8, where the density of coiled segments and the mobility as a function of the ratio of loop creation and annihilation rates c/a are shown. At a high ratio of creation to annihilation rates c/a, the chain is dense with stretched segments, and the mobility is low. At low c/a, there are few stretched segments that can move, and the mobility is again low. Around $c/a=1$, where the density of coiled segments is around one-half, the mobility is at a peak. The simulations show similar qualitative behaviors. The mean-field mobility overestimates the full model mobility by a factor of about 2. This is probably due to processes that impede the motion, such as hooking and pair creation in the bulk of the chain and not only at the head and tail, that are neglected in the mean-field treatment.

IV. ZERO-FIELD CASE

We now turn to the case of zero electric field. This case is important as a question in classical polymer physics [23,24]:

what is the effect of loops on the statics and dynamics of a chain in a gel or melt at equilibrium? In addition, the zero-field diffusion can be related to the low-field electrophoretic mobility via the Einstein-Nernst relations.

The zero-field case offers a significant simplification in the model: tension can be ignored in this case, and the model described in Sec. II is used, with $q=p$, $c=c'$, and $a=a'$. The probability of a given configuration C, $P(C)$, is governed by the Master equation

$$dP(C)/dt=\sum_{C'}\{W(C'\rightarrow C)P(C')-W(C\rightarrow C')P(C)\}, \tag{15}$$

where $W(A\rightarrow B)$ is the rate of transition from configuration A to B. A solution to the master equation is found which satisfies detailed balance. Each move which preserves the number of stretched segments, such as $+0\rightarrow 0+$, is exactly balanced by its reverse move. Moves where loops are created or annihilated are balanced by the reverse move, with an extra factor related to the creation and annihilation rates. A configuration A which has a 00 at a certain bond, can, in a single move, go to or be reached from only two configurations B and B', which are exactly the same as A except that they have either a $+_{\sqcup}-$ or a $-_{\sqcup}+$ at the bond. The solution for the probability of configuration C is

$$P(C)=N(L)^{-1}(c/a)^{h(C)}, \tag{16}$$

where c/a is the ratio between loop creation and annihilation rates, and $h(C)$ is the total number of loops in the configuration C. In the steady state, all configurations have equal probability, up to a factor depending only on the total number of loops in the configuration. This solution is remarkable in that, although there are strong interactions between different loops, the probability of each configuration depends only on the number of loops and not their relative positions and sizes. The normalization factor $N(L)=\Sigma_C(c/a)^{h(C)}$ is connected to the number of allowed configurations (only configurations with nested loops are allowed, as shown in Fig. 3). $N(L)$ satisfies the recursion relation

$$N(L)=N(L-1)+(2c/a)\sum_{l=0}^{L-2}N(l)N(L-2-l). \tag{17}$$

The terms on the right-hand side can be understood as follows: given a ring of size L, choose a site. The first term corresponds to the case where the site contains a 0, and thus the configurations of loops can be mapped to a ring of size $L-1$ by deleting the site. The second term is the case where the site is a member of a loop with its pair at a distance of $l+1$ sites (a loop of size l). The factor 2 in Eq. 17 is due to the two possible assignments of $+$ and $-$ charges to a loop pair, which have equal probabilities in the absence of an electric field. The values $N(0)=N(1)=1$ are supplemented to this recursion relation. Solving for the asymptotic form for $N(L)$ at $L\gg 1$, we consider the function $u(L)=\eta^{-L}N(L)$. For sufficiently large η it has a finite integral. Using a Laplace transform of $u(L)$, $g(s)=\Sigma_{L=0}^{\infty}u(L)e^{-sL}$, in the recursion relation Eq. (17), we find [33]

$$g(s)=\frac{1-e^{-s}\eta^{-1}+\sqrt{(e^{-s}\eta^{-1}-1)^2-4(2c/a)e^{-2s}\eta^{-2}}}{2(2c/a)\eta^{-2}e^{-2s}}. \tag{18}$$

The smallest value of η for which $g(0)=\Sigma u(L)$ exists is $\eta=2\sqrt{2c/a}+1$. At this value of η, for small s, $g(s)\approx g_0+g_1 s^{1/2}$. This corresponds to the following asymptotic form of the partition sum at $L\gg 1$:

$$N(L)=N_0 L^{-3/2}(2\sqrt{2c/a}+1)^L, \tag{19}$$

with

$$N_0=(4\sqrt{\pi}c/a)^{-1}(1+2\sqrt{2c/a})[\sqrt{2c/a}+4c/a]^{1/2}. \tag{20}$$

This allows a derivation of steady-state densities, such as ρ, the density of coiled segments (0's). This density is given from the construction of the recursion relation Eq. (17) simply by those configurations at which a given site is 0, compared to the total weight of the configurations:

$$\rho=N(L-1)/N(L)=(2\sqrt{2c/a}+1)^{-1}. \tag{21}$$

The loop size distribution, $n(l)$, defined as the probability that a selected site belongs to a loop of size l, is $n(l)=N(l)N(L-2-l)/N(L)$ [see Eq. (17)]. Thus, for $1\ll l\ll L/2$,

$$n(l)\approx N_0 l^{-3/2}. \tag{22}$$

This suggests that the ring polymer adopts a ramified fingered shape, with a power-law spectrum of finger sizes.

A. Average ring size

The exact solution also allows a calculation of the mean size of the ring at zero field. The radius of gyration serves as a convenient measure of the ring size: it is defined as the mean-squared distance between two sites (i.e., the sum of number of $+$ sites minus the number of $-$ sites between i and j squared, averaged over all configurations and all i and j). To evaluate the radius, we define the function

$$G(i)=\sum_C R_C^2(i)P(C), \tag{23}$$

where

$$R_C^2(i)=\left(\sum_{k=1}^{i}\phi_k\right)^2, \tag{24}$$

where ϕ_k is the state of site k in configuration C. That is, $G(i)$ is the average over all configurations of the squared distance between the two ''test sites'' 1 and i. The radius of gyration R is simply given by the root of the mean of $G(i)$,

$$R^2=L^{-1}\sum_{i=1}^{L}G(i). \tag{25}$$

We construct a recursion relation for $G(i)$, noting that the only contribution that does not average to zero is from un-

closed loops in the interval between the sites. Since there is no field, each site on a loop can be a + or a − with equal probability. The mean-squared distance, averaged over all assignments of + and − to the loops, is just the number of unclosed loops. To build a recursion relation for $G(i)$, we go from an interval of size $i-1$ to size i. Thus, to the interval of sites $1 \ldots i-1$ we add one site i, which may either be a 0, belong to a loop that closes outside the interval, or close one of the open loops in the interval. Thus we divide all possible configurations into three groups: C_0, in which site i is in a 0 state; C_1, in which site i belongs to a loop that closes outside the interval; and configuration C_2, in which site i pairs with a site inside the interval, thus closing a loop. In configuration C_0, $R_C^2(i)=R_C^2(i-1)$. In configuration C_1, $R_C^2(i)=R_C^2(i-1)+1$. In configuration C_2, $R_C^2(i)=R_C^2(i-1)-1$. Thus

$$G(i)=\sum_C R_C^2(i-1)P(C)+\sum_{C_1} P(C)-\sum_{C_2} P(C). \tag{26}$$

This leads to the recursion relation

$$G(i)=G(i-1)+(2c/a)\left[\sum_{l=i-1}^{L-2} N(l)N(L-2-l) - \sum_{l=0}^{i-2} N(l)N(L-2-l)\right] \Big/ N(L). \tag{27}$$

The boundary condition is $G(1)=1-N(L-1)/N(L)$, since the mean-squared displacement due to a single site is just the density of uncoiled segments $1-\rho$. $G(i)$ rises to a peak when $i=L/2$, and then drops off to 0 at $i=L$, because the ring is closed, and going around the ring the mean displacement must go to zero. Going to the continuum limit, and using the symmetry of $G(i)$ around $i=L/2$, we find

$$dG(i)/di=(2c/a)N(L)^{-1}\int_i^{L-i} N(l)N(L-l)dl. \tag{28}$$

For large i, using the asymptotic form of $N(L)$ found above [Eq. (19)], the integrals involved in calculating $G(i)$ can be performed analytically. This yields

$$G(i)=8(2c/a)N_0\sqrt{i}\sqrt{L-i}/\sqrt{L}, \tag{29}$$

showing that the mean maximal excursion of the ring is $G(L/2)\propto\sqrt{L}$. Integrating over $G(i)$, one obtains

$$R=\sqrt{\pi(2c/a)N_0}L^{1/4}. \tag{30}$$

This scaling is valid for long chains. The radius for finite chains can be readily found from the recursion relations (17) and (27). Thus the ring adopts a much more compact configuration than the linear, reptating chain, in which $R\propto L^{1/2}$. This form is valid for chains small enough that excluded volume effects can be neglected [25,31]. An intuitive argument predicted the $R\sim L^{1/4}$ scaling [26,27], by mapping the ring to a randomly branched graph. The exact solution of present model allowed us to derive this scaling exactly, from a steady state of a dynamic model.

B. Dynamics of a ring

The solution for the steady state allows a rather accurate approximation for the polymer dynamics. We consider the motion of a marked loop on the ring. We define $P(l,t)$ as the probability of finding the loop at size l at time t. The loop can grow if there is a 0 adjacent to the loop from the outside, and it can shrink if there is a zero adjacent to the loop from inside. We make the approximation that these probabilities are given by the corresponding steady state probabilities. This approximation is a good one for large loops. This is because the motion of the loops is diffusive, and hence many configurations of the ring segments inside and outside the marked loop are sampled on the time scale of the effective loop motion. The evolution equation for the size of the marked loop $P(l,t)$ is

$$\partial P(l,t)/\partial t=\rho_i(l+1)P(l+1,t)+\rho_o(l-1)P(l-1,t) - [\rho_i(l)+\rho_o(l)]P(l,t), \tag{31}$$

where $\rho_i(l)$ and $\rho_o(l)$ are the probabilities of a zero adjacent to the size-l loop from the inside and outside, respectively (a microscopic rate constant has been factored out of the equation so that each move take one time unit). At the boundaries, the equations have terms corresponding to the annihilation of the loop, which is possible when it is of size $l=0$ or $l=L-2$:

$$\partial P(0,t)/\partial t=\rho_i(1)P(1,t)-[a+\rho_o(0)]P(0,t), \tag{32}$$

$$\partial P(L-2,t)/\partial t=\rho_o(L-3)P(L-3,t) - [a+\rho_i(L-2)]P(L-2,t). \tag{33}$$

The main idea of the present approximation is to use the exact steady-state solution to estimate the probabilities of motion for the loop. This yields

$$\rho_i(l)=N(l-1)/N(l)\sim\rho(1+\tfrac{1}{2}l^{-1}), \tag{34}$$

$$\rho_o(l)=N(L-l-1)/N(L-l)\sim\rho[1+\tfrac{3}{2}(L-l)^{-1}], \tag{35}$$

where the asymptotic forms are valid at $l\gg 1$ and $L-l\gg 1$, and $\rho=(2\sqrt{2c/a}+1)^{-1}$. Note that smaller loops have on average more zeros inside them than larger loops. This is an entropic effect, due to the larger number of loop-pairings in a large loop. This creates a bias for small loops to shrink, an effect that has important consequences for the ring dynamics, as shown below.

In order to analyze the scaling of Eq. (31), it is convenient to turn to a continuum form

$$\partial P(l,t)/\partial t=\rho\nabla^2 P(l,t)+\rho\nabla[U(l)P(l,t)] \tag{36}$$

supplemented with appropriate boundary conditions (the exact form of the boundary conditions do not affect the scaling results obtained below). The potential, due to Eqs. (34) and (35),

$$U(l)=\tfrac{3}{2}[l^{-1}-(L-l)^{-1}], \tag{37}$$

corresponds to the bias of small loops to shrink. Consider the case of a marked loop created at time $t=0$. Thus the initial conditions are $P(l,t=0)=\delta(l=0)$. We define

$$F(l)=\int_0^\infty P(l,t)dt, \tag{38}$$

$$T(l)=\int_0^\infty tP(l,t)dt. \tag{39}$$

Thus the mean lifetime of the marked loop is

$$\tau=\int_0^\infty T(l)dl \Big/ \int_0^\infty F(l)dl. \tag{40}$$

Ordinary differential equations for $T(l)$ and $F(l)$ may be easily formed by appropriately integrating over Eq. (36),

$$-P(l,t=0)=\nabla^2 F(l)+\nabla[U(l)F(l)], \tag{41}$$

$$-F(l)=\nabla^2 T(l)+\nabla[U(l)T(l)]. \tag{42}$$

These equations are exactly solvable, yielding rather complicated expressions. However, to understand the scaling form of the solutions, it is useful to consider a simpler potential of the form $U=u_0/l$, which is equivalent to the full potential Eq. (37) at $l \ll L$, with $u_0=\frac{3}{2}$. Plugging in power law forms for F and T in Eqs. (41) and (42), we find $F(l)\sim l^{-u_0}$ and $T\sim l^{2-u_0}$. For $u_0=\frac{3}{2}$, $\int_0^\infty F(l)dl\sim F(0)$ and $\int_0^\infty T(l)dl\sim L^{3/2}$, yielding, for long chains,

$$\tau\sim\tau_0 L^{3/2}. \tag{43}$$

The same asymptotic result is found using the full potential of Eq. (37). The lifetime of a given marked loop is much shorter than that expected from a simple diffusion argument, $\tau\sim L^2$ (which corresponds to using no potential, $U=0$, in the above calculation). This is due to the entropic bias of small loops to shrink, which compels loops to spend less time in ''random walk'' motion as compared to the pure diffusion case. Note that the power-law exponent 3/2 in Eq. (43) is related directly to the prefactor of the effective potential that is derived from the detailed steady-state solution.

From this result, one can readily derive the scaling of the ring center of mass diffusion coefficient D, using a classical scaling argument [11]. Essentially, diffusion proceeds by the transport of loops along the ring. Each loop takes a time $\tau\sim L^\theta$ to travel a distance of order $R(L)\sim L^\nu$, the linear size of the polymer. If there were only one loop on the chain at any time, the center of mass diffusion constant D_0 would obey

$$D_0\tau=(R(L)/L)^2, \tag{44}$$

where the right hand side represents the mean-square displacement of the center of mass arising from the transport of one loop across a distance R. In reality, the number of loops present at any time is proportional to L. Hence the center of mass diffusion constant D scales as

$$D\sim LD_0\sim L^{2\nu-\theta-1}\sim L^{-2}, \tag{45}$$

where the values $\nu=\frac{1}{4}$ and $\theta=\frac{3}{2}$ were used. The result $D\sim L^{-2}$ is consistent with the simulations and intuitive arguments of Ref. [25]. It is remarkable that the diffusion coefficient scaling is the same as in a linear reptating chain [11], though the microscopic ''walker'' responsible for the motion has very different dynamics. In the case of a linear reptating chain, the exponents for the chain size and walker lifetime, $\nu=1/2$ and $\theta=2$, are different from the ring case, but they combine to give the same scaling for D. The longest relaxation time, in which the ring diffuses about one average ring size, scales as $T_{\max}\sim L^{5/2}$ (compare to the linear reptating chain result $T_{\max}\sim L^3$) .

The relaxation behavior is very different from that of a linear reptating chain [25]. In the linear reptating chain, for most structures to relax, the head of the chain must reptate and free them, a process takes of the order of the longest relaxation time $T_{\max}\sim L^3$. In contrast, the loop mechanism allows most structures to relax very quickly.

V. CONNECTION WITH SPONTANEOUS SYMMETRY BREAKING IN 1D

In this section, we discuss the models of gel electrophoresis in the context of systems that display spontaneous symmetry breaking (SSB) in one dimension (1D). It is well known that in thermal equilibrium, symmetry breaking and long-range order cannot appear in 1D systems with short-range interactions. Recently, a simple nonequilibrium model that displays SSB in 1D was presented [34]. The Rubinstein-Duke [9] reptation-tube model offers an additional interesting example of a 1D system with short-range interactions which displays symmetry breaking. In this model, symmetry breaking has a particularly simple physical meaning. Consider a linear DNA chain with no tension or loops. It is typically aligned with the field [9]. There are two symmetric configurations: either segment number 1 is at the chain head, or segment number L is at the chain head. A finite chain eventually flips between these two configurations. The flipping time, however, grows very quickly with the chain size: in order to flip, the tail must reptate an order of L steps against the field, and the rest of the chain must follow it, and thus the flipping time goes as $\sim e^{\alpha L^2}$ with some constant α. The chain is therefore effectively stuck in one of the two configurations and symmetry is broken in the thermodynamic limit.

In this example, as in the model of Ref. [34], the mechanism permitting spontaneous symmetry breaking depends on the presence of boundaries (i.e., the existence of a chain head and tail) and on a conservation law in the chain bulk (the number of $+$ and $-$ particles is conserved by the bulk dynamics when loops are not permitted). The latter is seen to be important by allowing loops, as in the present model (without tension which corresponds to long-ranged interactions). Loops amount to pair creation and annihilation in the bulk, and break the conservation law. Adding loops also cancels the SSB: the chain is typically stuck in a symmetric hooked state (Sec. III A, Fig. 5).

We note that an interesting case of SSB in a 1D system, with periodic boundary conditions and with no bulk conservation of the order parameter has been presented [35].

VI. DISCUSSION

The role of tension and loops in the dynamics of ring-shaped DNA gel electrophoresis is studied. A microscopic model, which adds tension and loops to the reptation model of Rubinstein and Duke, was proposed. The model is similar to reaction-diffusion models, with the addition of a interesting hierarchical pairing which represents the loop fingers.

We predict that the mobility of open-circular DNA should saturate much as in linear chains. Tension serves to stabilize a quasilinear conformation of the ring. In this regime, there are many coiled DNA segments, screening the effects of tension. The screening of tension by coiled segments is essential for explaining the success of reptation models for linear DNA fragments [10,32], which neglect both loops and tension. It is suggested that tension and loops have, to a certain extent, canceling effects. It is thus important to include both effects in models of loop-mediated polymer dynamics. Some of the qualitative features of the motion of the ring are captured by a simple mean-field theory.

The present predictions are difficult to check in standard electrophoresis experiments in agarose gels in which the DNA rings become hooked on dangling ends in the gel (''hoop in stick'' effect, Sec. III B). An experimental situation which eliminates the effects of dangling ends is offered by the microlitthographic arrays of posts introduced by Volkmuth and Austin [28]. These arrays were used to study electrophoresis of linear DNA, which could be observed by fluorescence microscopy. Since these two-dimensional (2D) arrays have a floor and a ceiling attached to the posts, a ring-shaped DNA cannot become impaled by a post. Thus the hoop in stick effect is negated. The present work predicts that the mobility of plasmids in such an obstacle array should saturate at a finite value, and not decrease exponentially with the ring size as in standard gels with dangling ends.

In addition, agarose gels exhibit a very broad distribution of pore sizes. The present model pertains more closely to experiments on regular lattice, since the broad distribution of pore sizes in standard agarose gels might well affect the dynamical features and scaling laws discussed in this paper.

The model is also applied to study dynamics in zero field. The solution of the model in this case allows an exact foundation of some known scaling properties of ring polymers. The main effect of loops on the static chain properties are to allow many undulations and wiggles per unit contour length. As a result, the ring adopts much more compact configurations (average size $R \sim L^{1/4}$) than in the reptation case (where $R \sim L^{1/2}$). The dynamics have been studied using an interesting approximate equation of motion for marked loops. This equation seems to be a useful basis for analytical study of the effect of loops on polymer dynamics. The lifetime of a loop was found to scale as $\tau \sim L^{3/2}$, which is shorter than expected from pure diffusion $\tau \sim L^2$. This is due to an entropic bias of small loops to shrink and be annihilated. The diffusion coefficient is found to scale as in the reptation case, $D \sim L^{-2}$, though the behavior of the microscopic walker is different in the reptation and ring cases. The relaxation spectrum is very different, with most structures relaxing on short time scales. These results were obtained for ring-shaped polymers, but should also be applicable to long linear chains in which loop creation in the bulk is allowed. An exact solution of the steady state is also possible in this case, showing a crossover between reptation and loop behavior as a function of polymer length. This solution, as well as a more detailed study of the zero-field dynamics, will be presented in a future publication. Finally, we note that the physically intuitive treatment of chain tension presented here may be useful also for describing different systems in which polymers in a melt or obstacle array move under external forces.

ACKNOWLEDGMENTS

We thank R. Austin, S. Leibler, S. Sandow, and L. Ulanovski for helpful discussions. This work was supported by the Minerva Foundation, Munich.

[1] B. Alberts, D. Bray, J. Lewis, M. Raff, K. Roberts, and J. D. Watson, *Molecular Biology of the Cell*, 3rd ed. (Garland, New York, 1994).
[2] D. C. Schwartz and C. R. Cantor, Cell **37**, 67 (1984).
[3] G. F. Carle, M. Frank, and M. V. Olson, Science **232**, 65 (1986).
[4] O. J. Lumpkin, P. Dejardin, and B. H. Zimm, Biopolymers **24**, 1573 (1985).
[5] G. W. Slater and J. Noolandi, Phys. Rev. Lett. **55**, 572 (1985).
[6] M. Doi, T. Kobayashi, Y. Makino, M. Ogawa, G. W Slater, and J. Noolandi, Phys. Rev. Lett. **61**, 1893 (1988).
[7] M. Rubinstein, Phys. Rev. Lett. **59**, 1946 (1987).
[8] T. A. J. Duke, Phys. Rev. Lett. **62**, 2877 (1989).
[9] T. A. J. Duke, J. Chem. Phys. **93**, 9052 (1990).
[10] T. Duke, J. L. Viovy, and A. N. Semenov, Biopolymers **34**, 239 (1994); C. Heller, T. Duke, and J. L. Viovy, *ibid.* **24**, 249 (1994);
[11] J. P. de Gennes, J. Chem. Phys. **55,** 572 (1971).
[12] J. M. Deutsch, Science **249**, 922 (1988).
[13] S. Gurrieri, E. Rizzarelli, D. Beach, and C. Bustamente, Biochemistry **29**, 3396 (1990).
[14] B. H. Zimm, J. Chem. Phys. **94**, 2187 (1991).
[15] S. B. Smith, C. Heller, and C. Bustamente, Biochemistry **30**, 5264 (1991).
[16] T. A. J. Duke and J. L. Viovy, Phys. Rev. Lett. **68**, 542 (1992).
[17] W. D. Volkmuth, T. Duke, M. C. Wu, R. H. Austin, and A. Szabo, Phys. Rev. Lett. **72**, 13 (1994).
[18] The term open circular refers to ring-shaped DNA which is not supercoiled (closed circular). Open-circular DNA is obtained from supercoiled DNA by a nicking procedure, which removes base pairs from one of the strands, allowing the double-stranded DNA to swivel and release the torsion which caused it to supercoil [19].
[19] S. Mickel, V. Arena, and W. Bauer, Nucleic Acids Rec. **4,** 1465 (1977).
[20] P. Serwer and S. Hayes, Electrophoresis **8,** 244 (1987).
[21] S. Levene and B. H. Zimm, Proc. Natl. Acad. Sci. U.S.A. **84**, 4054 (1987).

[22] M. Wang and E. Lai, Electrophoresis **16**, 1 (1995).
[23] J. Klein, Macromolecules **19**, 105 (1986).
[24] M. E. Cates and J. M. Deutch, J. Phys. **47**, 2121 (1986).
[25] S. P. Obukhov, M. Rubinstein, and T. Duke, Phys. Rev. Lett. **73**, 1263 (1994).
[26] B. H. Zimm and W. H. Stockmayer, J. Chem. Phys. **17**, 1301 (1949).
[27] A. R. Kholkov and S. K. Nechaev, Phys. Lett. **112A**, 156 (1985).
[28] W. D. Volkmuth and R. H. Austin, Nature **358**, 600 (1992).
[29] The quasilinear conformation is represented in the model by a phase-separated distribution of charges, where half of the lattice is rich with + sites and the other half rich with − sites, as shown in Fig. 6(a), along with the appropriate pairing into loop pairs. Typically the conformation also includes many 0 sites, small branching subloops, etc.
[30] E. M. Sevick and D. R. M. Williams, Phys. Rev. E **50**, 3357 (1994).
[31] G. Parisi and N. Sourlas, Phys. Rev. Lett. **46**, 871 (1981).
[32] G. T. Barkema and G. Schutz (unpublished).
[33] This equation represents the positive root of a quadratic equation for $g(s)$. The negative root corresponds to a nonphysical solution in which $N(L)$ is negative at large L.
[34] M. R. Evans, D. P. Foster, C. Godréche, and D. Mukamel, Phys. Rev. Lett. **74**, 208 (1995); J. Stat. Phys. **80**, 69 (1995); C. Godréche, J. M. Luck, M. R. Evans, D. Mukamel, S. Sandow, and E. R. Speer, J. Phys. A **28**, 6039 (1995).
[35] U. Alon, M. R. Evans, H. Hinrichsen, and D. Mukamel, Phys. Rev. Lett. **76**, 2746 (1996).